Modulation of Cellular Mechanics during Osteogenic Differentiation of Human Mesenchymal Stem Cells

Igor Titushkin and Michael Cho
Department of Bioengineering, University of Illinois, Chicago, Illinois

ABSTRACT Recognition of the growing role of human mesenchymal stem cells (hMSC) in tissue engineering and regenerative medicine requires a thorough understanding of intracellular biochemical and biophysical processes that may direct the cell's commitment to a particular lineage. In this study, we characterized the distinct biomechanical properties of hMSCs, including the average Young's modulus determined by atomic force microscopy (3.2 ± 1.4 kPa for hMSC vs. 1.7 ± 1.0 kPa for fully differentiated osteoblasts), and the average membrane tether length measured with laser optical tweezers (10.6 ± 1.1 μm for stem cells, and 4.0 ± 1.1 μm for osteoblasts). These differences in cell elasticity and membrane mechanics result primarily from differential actin cytoskeleton organization in these two cell types, whereas microtubules did not appear to affect the cellular mechanics. The membrane-cytoskeleton linker proteins may contribute to a stronger interaction of the plasma membrane with F-actins and shorter membrane tether length in osteoblasts than in stem cells. Actin depolymerization or ATP depletion caused a two- to threefold increase in the membrane tether length in osteoblasts, but had essentially no effect on the stem-cell membrane tethers. Actin remodeling in the course of a 10-day osteogenic differentiation of hMSC mediates the temporally correlated dynamical changes in cell elasticity and membrane mechanics. For example, after a 10-day culture in osteogenic medium, hMSC mechanical characteristics were comparable to those of mature bone cells. Based on quantitative characterization of the actin cytoskeleton remodeling during osteodifferentiation, we postulate that the actin cytoskeleton plays a pivotal role in determining the hMSC mechanical properties and modulation of cellular mechanics at the early stage of stem-cell osteodifferentiation.

INTRODUCTION

The bone-marrow-derived mesenchymal stem cells (MSCs) are considered to be the pluripotent cells that can be expanded in vitro and differentiated into many tissue-specific lineages, including osteoblasts, adipocytes, muscle cells, and others (1–3). The use of MSCs not only eliminates controversial ethical issues associated with embryonic stem cells but also is suitable for engineering bone, cartilage, muscle and other connective tissues. However, realization of the promising potential of stem cells for tissue engineering requires a proper characterization of their unique biological, biochemical, proteomic, and biomechanical properties that are yet to be fully elucidated. The mechanical properties, such as cytoskeleton organization and elasticity, membrane tension, cell shape, and adhesion strength, may play an important role in cell fate and differentiation (4–6). Matching mechanical properties of hMSC to those of fully differentiated cells is crucial for development of functional load-bearing connective tissue. Moreover, manipulation of the cellular mechanics may increase the efficacy of cell differentiation, integration with scaffolds, and eventual tissue substitute maturation.

One of the most important cellular mechanical parameters is cell elasticity. Cell compliance is essential, as the cells must undergo multiple deformations without losing their integrity. Cell elasticity is known to be determined by cytoskeletal elements, including microfilaments, microtubules, and intermediate filaments (7,8). One comprehensive model of the cell cytoskeleton organization is the tensegrity model (9,10). In this model, actin microfilaments and microtubules represent tension-bearing and compression-bearing elements, respectively. Such stress-supported structure can mimic a number of features observed in living adherent cells, including prestress-induced stiffening and strain hardening (11–14). However, no single theoretical model can describe the vast variation in cytoskeleton mechanics due to cell-type-dependent cytoskeleton composition, and molecular organization and its regulation (14–16). A complete theoretical description of the diverse cytoskeleton functions still remains elusive. Substantial structural and functional differences of cytoskeletons in cells of the same mesodermal origin (myocytes, osteoblasts, endothelial cells, kidney cells, etc.) imply that the cytoskeleton may also participate in cell differentiation. Besides providing cell-shape stability, the cytoskeleton plays an important role in signaling pathways that regulate intracellular processes and protein expression in response to a changing biomechanical environment. The role of cytoskeleton as a mechanotransducer has been articulated in the studies of cellular responses to changing substrate stiffness, cell shape, stretching, and shear stress (6,17–19). Several cytoskeleton signaling pathways include the Rho family GTPases (e.g., Rho, Cdc42, Rac). Complex interactions between these molecular switches, triggered by external signals, cause activation of numerous downstream target proteins. The result is a global structural rearrangement of the cytoskeleton itself or altered gene transcription profiles

Submitted February 28, 2007, and accepted for publication June 13, 2007.

Address reprint requests to Dr. Michael Cho, Dept. of Bioengineering, University of Illinois, Chicago, 851 S. Morgan St. (M/C 063), Chicago, IL 60607. Tel.: 312-413-9424; Fax: 312-996-5921; E-mail: mcho@uic.edu.

Editor: Marileen Dogterom.

0006-3495/07/11/3693/10 $2.00

doi: 10.1529/biophysj.107.107797

affecting cell adhesion, secretion of extracellular matrix components, and cell metabolic activity (20,21).

Several techniques that have been successfully employed to study the cell elastic properties include micropipette aspiration, magnetic twisting cytometry, and atomic force microscopy (22–24). The latter method can be used to image live cells and probe their mechanical properties in physiological conditions in a nondestructive manner (25). It also allows elastic data acquisition with a high spatial resolution in real time to follow the fast changes in cell mechanics. In these experiments, the atomic force microscope (AFM) cantilever serves as a microindenter to poke the cell, and further analysis of force-indentation data yields the local Young's modulus. In addition, the AFM indentation technique can be used to characterize the viscoelastic behavior of the cell cytoskeleton, including viscosity, loss and storage moduli, and stress relaxation times (26–28).

Another important mechanical component of the cell is its plasma membrane. Not only does it separate the interior of the cell from the outer environment, it also participates in the inward-outward trafficking, cell adhesion to extracellular matrix, motility, and cell-cell interaction. Due to the important role of the membrane in many cellular functions, it is likely involved in the intricate interplay of events accompanying cell differentiation. Membrane surface tension is known to regulate many intracellular events, and multiple mechanisms are involved in its maintenance (29–31). Many adherent cells store extra membrane—in the form of ruffles, folds, undulations, and caveolae—that is often referred to as the membrane reservoir (32). The membrane reservoir is intended to buffer fast, small surface-tension fluctuations. Larger variations in the membrane area are accommodated by lipid-material recycling mechanisms. The existence of a membrane reservoir in many cell types has been repeatedly demonstrated in experiments using membrane tether extraction. When a micron-sized latex bead attached to the membrane is pulled away from the cell, a thin, hollow lipid tether is formed. A constant force required for tether elongation indicates that the lipid material is being pulled from the available membrane depot (32,33). The membrane reservoir size is cell-type-dependent and may be regulated by the membrane's composition, mechanical rigidity, interaction with cytoskeleton, and lipid bilayer turnover. We have shown previously that the membrane reservoir in hMSC is much larger than in fully differentiated cells (34). Our membrane tether extraction experiments suggest a stronger interaction between the plasma membrane and the underlying cytoskeleton in fibroblasts compared to stem cells. Tether extraction using laser optical tweezers (LOT) is perhaps the most accurate technique to quantitatively characterize membrane mechanics in many important processes, such as cell spreading, osmotic stress, endocytosis, and membrane repair (29,30,35).

In this study, we compared the membrane and cytoskeleton mechanics of hMSCs to those measured from differentiated osteoblasts, default hMSC descendants. Based on the mechanical differences we have quantitatively determined in these two cell types, potential mechanisms of regulation of membrane mechanics and cytoskeleton elasticity have been postulated. By investigating the dynamical changes in the hMSC mechanics upon osteogenic differentiation in vitro by soluble biochemical factors, we formulated a model in which the intracellular F-actin organization is pivotal for modulating both cellular-cytoskeleton and plasma-membrane mechanics of differentiating hMSCs.

MATERIALS AND METHODS

Cell culture, differentiation assays, and drug treatment

Human mesenchymal stem cells were obtained from the Tulane Center for Gene Therapy (New Orleans, LA). Based on the flow cytometry results, these stem cells showed negative staining for CD34, CD36, CD45, and CD117 markers (all $<2\%$), and positive staining for CD44, CD90, CD166, CD29, CD49c, CD105, and CD147 markers (all $>95\%$), indicating a minimal heterogeneity in cell population. Normal human fetal osteoblasts (hFOB 1.19) were obtained from American Tissue Culture Collection (Manassas, VA). Cells were grown in Dulbecco's modified Eagle's culture medium with 15% fetal bovine serum, L-glutamin, and antibiotics. Two days before the experiments, cells were harvested and plated on glass coverslips. Cells were gently rinsed with phosphate-buffered saline and mounted on the AFM chamber or LOT coverglass chamber. To differentiate hMSCs into bone cells, we used the osteogenic induction medium containing 10 nM dexamethasone, 50 μM L-ascorbic acid, and 20 mM β-glycerophosphate. The proper osteogenic differentiation was verified by specific osteogenic markers such as osteocalcin, osteopondin, alkaline phosphatase, calcium mineralization, and gene expressions (data not shown (36)). hMSCs between passages 3 and 9 were used for all experiments.

To study the effect of drugs on cellular mechanics, cells were incubated at 37°C for 30 min in reagent solution: cytochalasin D (5 μM), nocodazole (5 μM), and antimycin A (10 μM). All drugs were purchased from Sigma-Aldrich (St. Louis, MO).

Measurement of cell elasticity using the AFM microindentation test

The live-cell elasticity was measured with a Novascan atomic force microscope (Novascan Technologies, Ames, IA) mounted on an inverted Nikon microscope (Tokyo, Japan). A piezoelectric scanner with a maximum XY range of 80×80 μm and vertical z range of 7.3 μm was used. Soft silicone nitride cantilevers (Veeco, Santa Barbara, CA), 100 μm long, were calibrated by the thermal fluctuation method in the air (37–39), with a typical spring constant value of 0.12 N/m. Borosilicate glass beads (10 μm in diameter) glued onto the cantilever served as cell indentors. An isolated cell with normal morphology was identified using the optical microscope and the AFM cantilever probe was positioned over the cytoplasmic region of the cell between the nucleus and the cell peripheral margin. Each cell was mechanically probed with AFM at several locations over a 15×15 μm area, avoiding the cell's perinuclear region. The force curve was obtained by measuring the cantilever deflection (and, correspondingly, the applied force) at every vertical z-position of the cantilever as it approached and indented the cell. The cantilever descended toward the cell at a velocity of $\sim$2 μm/s until a trigger force of 3 nN was reached, which corresponded to 0.5–1 μm indentation depth, or $\sim$10–15% of the total cell height. A total of 50–60 cells of each type and experimental condition were used, with $\sim$15 force-distance curves acquired from each cell. The force-distance curves were collected and analyzed according to the Hertz model (40–42), which relates the loading force, F, with indentation depth δ:

$$F = \frac{4}{3}\frac{E}{(1-\nu^2)}\delta^{3/2}\sqrt{R},$$

where ν is the cellular Poisson's ratio, R is the radius of the spherical indentor (5 μm), E is the local Young's elastic modulus, and δ is the cell indentation depth. The cellular Poisson's ratio was assumed to be 0.5, which treats the cell as an incompressible material (42–44). The bidomain polynomial model (linear for precontact and Hertz's equation for postcontact, with adjustable contact point z_o) was fit to the experimental force curve using a standard least-squares minimization algorithm. The fit yielded two unknown parameters: the contact point of AFM probe with the cell at z_o and pointwise apparent elastic modulus E. Distributions for the measured E values were plotted, and the average Young's modulus for each cell type and experimental condition was calculated and subjected to t-test at an α level of 0.05.

Membrane tether extraction with LOT

Fluorescent polystyrene beads 0.5 μm in diameter with 515-nm emission (FluoSpheres, Molecular Probes, Eugene, OR) were covalently coated with mouse anti-CD29 antibodies and tightly bound to the cell membrane. The beads were used as handles for membrane tether extraction, as described earlier (34). An infrared Nd:YAG laser (1064 nm, continuous wave, with 0.5 W maximum incident power at the sample; SpectraPhysics, Mountain View, CA) with a Nikon microscope was used for particle optical trapping. The laser beam was focused in the cell surface with a 100× oil immersion microscope objective (PlanApo, NA 1.4), and this optical trap was moved in the focus plane by a system of two confocal lenses actuated by a high-precision motorized translator. Cells, laser, and fluorescent beads were imaged with a 16-bit CCD camera (Photometrics, Tucson, AZ) in the bright-field and epifluorescence modes.

To extract a membrane tether from the cell, a latex bead attached to the cell was chosen randomly and optically trapped. The bead was then displaced from its equilibrium position by moving the trap away from the cell at a constant speed of 1.5 μm/s. Tether growth was observed until the bead escaped from the trap. Elastic membrane tether formation was identified by quick retraction of the bead to its original position after escape from the trap. The total tether length was determined by tracking bead position using a MetaMorph image processor (Molecular Devices, Downingtown, PA). Typically, 35–40 beads from ~20 cells were analyzed for each experimental condition and cell type.

Immunostaining and confocal microscopy

To explore the cytoskeleton structure of normal and cytochalasin D and nocodazole-treated cells, samples were fixed in 3.7% formaldehyde and permeabilized in cold (−20°C) acetone for 3 min. Nonspecific binding sites were blocked using a 1% BSA solution for 30 min at room temperature. Intracellular actin filaments were stained with rhodamin-phalloidin (5 μM) for 30 min at room temperature (Molecular Probes) and microtubules were labeled with monoclonal anti-α-tubulin antibody conjugated to FITC (Sigma-Aldrich). Samples were imaged by a laser scanning confocal system (Radiance 2001MP, Bio-Rad, Hercules, CA) running on a Nikon TE2000-S inverted microscope with 60× Plan Apo objective (NA 1.4), blue Argon ion (488 nm), and green HeNe (543 nm) lasers. Emission filters (515/30 nm and 600/50 nm) were used to collect confocal images of microtubules and microfilaments, respectively.

RESULTS

Cytoskeleton elasticity of stem cells and osteoblasts

To characterize the elastic properties of the cells, we used the AFM indentation technique described in detail elsewhere (41,42,45). Although the Hertz model has been validated for the microindentation analysis of cell mechanical properties, care must by taken in interpreting the AFM indentation data. The Hertz model treats the tested sample as homogeneous, semi-infinite, isotropic, and linear elastic material. In contrast, intrinsic fibrillar cytoskeleton structure results in a spatial heterogeneity of the cell elasticity on a nanometer to micrometer scale (46). Distribution of the indenting load over a several-μm^2 area averages the contribution of multiple cytoskeleton fibers and makes the Hertz analysis more accurate. Indeed, the use of a spherical indenter 10 μm in diameter, compared to regular pyramidal sharp SiNi AFM tips, allows us to reduce experimental elastic data dispersion severalfold (data not shown). Further, to treat the cell as semi-infinite material, the deformations of the cell should be small enough that the measurements are not influenced by the cell boundary and underlying substrate. To minimize the effect of the glass substrate on the shape of the force curve, we used an indentation depth up to 500 nm (~10% of the average cell height) for data analysis. Another Hertz model assumption about the indentation depth (δ) being much less than the spherical indenter radius (R) is also met in these conditions. Finally, to exclude viscous effects of solution and the cell, the indenter was actuated at a low speed, ~2 μm/s. Hysteresis was quantified by subtracting the area under the indentation and retraction curves, which represents the viscous dissipation of energy into the cell. The hysteresis loop area was normalized to input energy (the area under the indentation curve). Calculated in this manner, hysteresis was ~15–20%, indicating that energy dissipation due to the material viscosity contribution is low at this probe velocity and force measurements are dominated by the cell's elastic behavior (43,47). A further decrease in speed did not result in significant changes of the force-curve shape or decline in hysteresis (see Supplementary Material for details). Thus, the Hertz model assumptions are adequately satisfied under our chosen experimental conditions.

Typical force curves and the average Young's moduli for hMSC and osteoblasts calculated using the Hertz model are presented in Fig. 1. Variation of data between different cells did not exceed the variation within an individual cell and is probably due to intrinsic variation of the local cell cytoskeleton elasticity. The average elastic modulus for hMSC, 3.2 ± 1.4 kPa, is almost twofold higher than that for osteoblasts, 1.7 ± 1.0 kPa (Fig. 1 *B*). Treatment of cells with cytochalasin D caused the elastic modulus to decrease to 0.7 ± 0.3 kPa in hMSCs and to 0.9 ± 0.5 kPa in osteoblasts. Interestingly, microtubule disruption with nocodazole caused only a minor, statistically insignificant decrease ($p = 0.05$) in cell elasticity in both cell types (Fig. 1). The residual elasticity after treatment with both drugs is statistically indistinguishable in both cell types and could have been provided by intermediate filaments and other intracellular components.

In a separate set of experiments, performed to assess the cell viability after AFM mechanical testing, all the cells

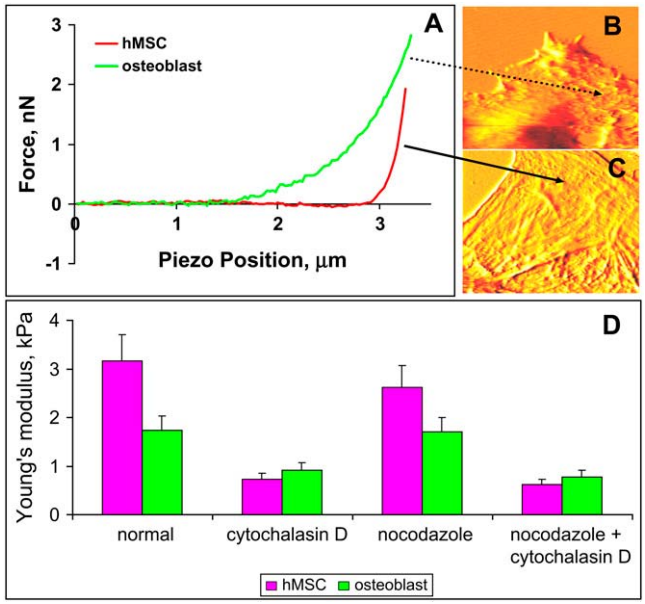

FIGURE 1 Measurements of cell elasticity with AFM microindentation. Live cell imaging and mechanical testing were conducted in phosphate-buffered saline with normal or drug-treated cells. (*A*) Typical force-distance curves obtained for normal osteoblasts (*B*) and stem cells (*C*). Measurements were performed on the area between the nucleus and the margin of the cell (*arrows*). The scan size of both AFM images is 40 × 40 μm. Note the higher contrast in hMSCs (*C*) than in osteoblasts (*B*) due to stronger, thicker stress fibers in the hMSC cytoskeleton. (*D*) Effect of cytoskeleton-destabilizing drugs on the average elastic modulus of the cells; ~600–800 force curves were acquired for each cell type and condition. There is no statistical significant difference at $p = 0.05$ between nocodazole and their corresponding controls.

within a designated area (700 × 700 μm) were indented (~40 cells). Viable/dead cells were counted using trypan blue staining. The cell viability of control cells not indented was >95% and did not change after AFM indentation (data not shown). Thus, cell manipulation with AFM does not appear to adversely affect cell viability.

Membrane tether extraction with LOT

Polystyrene beads tightly bound to the cell membrane were optically trapped and used as handles to form membrane tethers. The beads were conjugated to anti-CD29 antibodies that recognize β_1-integrins abundantly expressed at the cell surface of both hMSCs and osteoblasts. Binding specificity of antibody-coated probes has been verified in control experiments with noncoated beads; ~20–40% of membrane-associated beads were fluctuating on the cell surface, and could be trapped and moved away from the cell to produce a tether. The typical optical force-elongation curve exhibits a constant force of ~3 pN over the large course of tether growth (Fig. 2). A plateau on the force-distance profile suggests that additional membrane is being drawn from a buffered membrane reservoir (32). This membrane reservoir may be represented by ubiquitous membrane surface undulations such as ruffles, pits, and caveolae. To exclude the possibility of mechanical or structural changes in the cell due to laser-induced photodamage, we repeated experiments with selected beads with 1- to 2-min intervals with consistently reproducible results.

The average tether length in osteoblasts (4.0 ± 1.1 μm) was similar to that previously measured in fibroblasts (3.0 ± 0.5 μm) (34), but much lower than 10.6 ± 1.1 μm in undifferentiated stem cells, suggesting that the membrane mechanics in the fully differentiated musculoskeletal cells (e.g., fibroblasts, osteoblasts) may be the same. The inhibition of actin polymerization with cytochalasin D resulted in almost a 2.5-fold tether-length increase in osteoblasts, but had no effect on the tether length in stem cells. As we postulated earlier (34), this result may be due to a weak membrane-cytoskeleton interaction in hMSCs compared to fully differentiated cells. In many cell types, the membrane-cytoskeleton attachment is mediated by small protein linkers such as ezrin and myosin-I. The activity of these proteins is inhibited by energy depletion (48–51). ATP depletion had a minimal effect on tether length in hMSCs, but produced

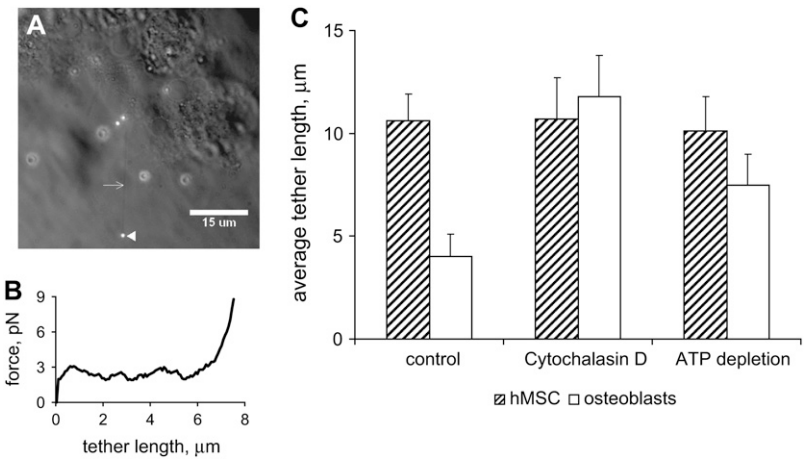

FIGURE 2 Membrane tether extraction with laser optical tweezers. (*A*) Fluorescent polystyrene beads coated with anti-integrin antibodies attached to a normal stem cell surface and pulled away with LOT (*arrowhead*) to extract a long thin membrane tether (*thin arrow*). (*B*) Force applied by LOT to the bead to form a tether. Force is constant for most of tether growth due to membrane pulling from the membrane reservoir (32). Upon reservoir depletion the maximum tether length is reached, the force sharply increases, and the bead escapes from the optical trap. (*C*) Effect of the membrane-cytoskeleton interaction on average membrane tether length in two cell types. All treatments produced a statistically significant ($p < 0.05$) tether length increase in osteoblasts, but not hMSCs.

rather longer tethers in osteoblasts (Fig. 2). This finding indicates a significant contribution of the protein linkers in the membrane-cytoskeleton interaction in fully differentiated osteoblasts. No changes in cell morphology or cytoskeleton structure were observed by ATP depletion.

Cytoskeleton organization in hMSCs and osteoblasts

Significant differences in cellular mechanics between hMSCs and osteoblasts may result from different cytoskeleton organization in these cells. Dual staining confocal microscopy was used to explore the cytoskeleton arrangements in the two cell types. Optical sections of fixed and adhered cells were recorded from ~1–2 μm above the substrate. Based on these confocal images, we observed no significant differences in the microtubule structure between the two cell types (Fig. 3). However, we found strikingly different features in actin organization. hMSCs demonstrated many thick actin bundles, or stress fibers, extending throughout the cytoplasm and terminating at focal contacts on the cell membrane. In contrast, osteoblasts had fewer stress fibers and showed, predominantly, a thin dense meshwork structure of actins. The average actin concentration, roughly estimated from the fluorescent images, appeared to be similar in both cell types. After cytoskeleton disruption, residual patches of actin left behind depolymerized stress fibers can distinctly be observed at the focal contact sites (Fig. 3 *B*).

Mechanical changes in hMSC during osteogenic differentiation

To study how the mechanics of stem cells change when they commit to the osteogenic lineage, we cultured hMSCs in the osteogenic induction medium and monitored alterations in cytoskeleton elasticity and membrane tether length. During osteogenic differentiation, both the elastic modulus and the average membrane tether length decreased and approached the values typical for fully differentiated mature bone cells (Fig. 4). For example, after a 10-day culture in the osteogenic medium, the Young's modulus of hMSCs dropped from 3.2 $\pm$ 1.4 kPa to 2.1 $\pm$ 0.9 kPa (only 23% higher than that of a normal osteoblast), and the average tether decreased from 10.6 $\pm$ 1.1 μm to 4.8 $\pm$ 1.0 μm (only 19% different from that of osteoblasts). Interestingly, neither mechanical parameter changes significantly until after day 3 of differentiation induction. This temporal correlation may be due to the cytoskeleton reorganization caused by differentiation, as actin arrangement appears to affect the two measured mechanical parameters. In control experiments with stem cells placed in the regular growth medium (Fig. 4) and osteoblasts in the osteogenic medium (data not shown), no significant changes of the mechanical properties were detected.

Actin cytoskeleton remodeling in differentiating hMSCs

As the actin structure in stem cells is much different from that in terminally differentiated osteoblasts, actin cytoskeleton remodeling is expected during hMSC differentiation into bone cells. Indeed, as osteogenic differentiation of hMSCs progresses, more and more stress fibers are replaced with a thinner actin network that is characteristic of mature osteoblasts (Fig. 5). The concentration of F-actins does not seem to change, as roughly estimated from fluorescence images. However, some thick actin bundles can still be found in the cells even after 10 days of osteodifferentiation. It

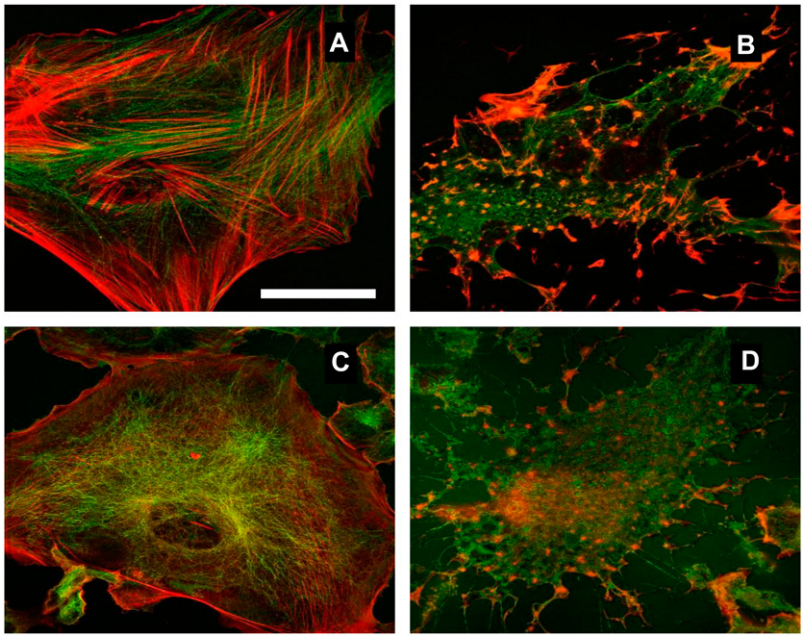

FIGURE 3 Cytoskeleton organization in undifferentiated hMSCs (*A* and *B*) and mature osteoblasts (*C* and *D*). In these confocal images, actins and tubulins were stained with rhodamine-phalloidin (*red*) and FITC-conjugated anti-α-tubulin antibody (*green*), respectively. Stem cells (*A*) have many thick actin bundles (stress fibers), unlike osteoblasts (C), which have a thinner actin filament meshwork. After treatment with cytochalasin D and nocodazole, the cytoskeleton is fully disintegrated (*B* and *D*), and patches of actins are left at the focal adhesion sites. Scale bar, 30 μm.

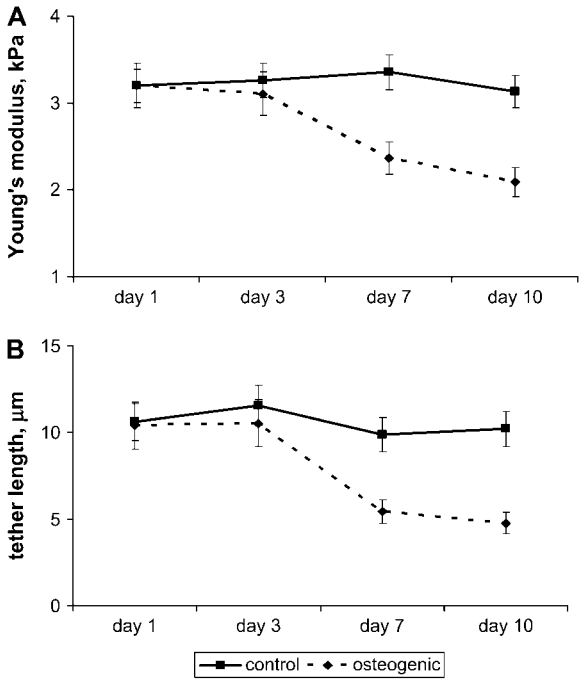

FIGURE 4 Alteration of cellular mechanical parameters during hMSC osteodifferentiation. Both the cell average Young's modulus (*A*) and average membrane tether length (*B*) decrease significantly ($p < 0.05$) with 7-day incubation in the osteogenetic medium (*dashed lines*). In control experiments, undifferentiated hMSCs were grown in regular culture medium for 10 days without significant mechanical changes (*solid lines*).

should be noted that typical molecular osteogenic markers are expressed only after 7–14 days of differentiation (52). Apparently, after a 10-day culture, cells are osteogenically committed, but likely not fully differentiated.

DISCUSSION

Biomechanics plays a very important role in cellular metabolism. Cell growth, proliferation, migration, adhesion, and differentiation all depend on and are regulated by cellular mechanical properties. Eukaryotic cells are known to respond to external mechanical stimuli by adjusting their biochemical and biomechanical properties (19,53). Therefore, a thorough understanding of cell mechanical parameters would be important in the development of cell manipulation techniques for cell biology, medicine, and tissue engineering.

One of the most significant mechanical parameters of the cell is its elasticity. Previously reported elastic moduli of connective tissue cells determined by AFM range between 0.1 and 100 kPa (26,43). This variation is probably not only due to cell type variability, but likely stems from different experimental conditions and analytical approaches used (25,41). Our measurements of the cell elastic moduli are comparable to the previously reported 1.6 ± 2.2 kPa for 3T3 fibroblasts (27), 1–2 kPa for osteoblasts (54), 1.8 ± 0.3 kPa for fibroblasts (55), 1.5–5.5 kPa for endothelial cells (46), and 0.3–30 kPa for bone marrow stromal cells (56). It should be noted that the apparent Young's moduli reported in this study were calculated in a simple quasielastic approximation, even though cells might also exhibit differences in viscous properties and possible nonlinear elastic behavior (43).

Cell-body elasticity is determined by the cell's cytoskeleton. The cytoskeleton is a dynamic structure capable of reorganization as required by cell type, specification, stage of development, and environmental conditions. For example, the cytoskeleton of MSCs differs considerably from that of bone cells in the polymeric actin structure. Whereas in hMSC actins are organized as thick bundles traversing the cell cytoplasm, in osteoblasts they are arranged as a thin dense

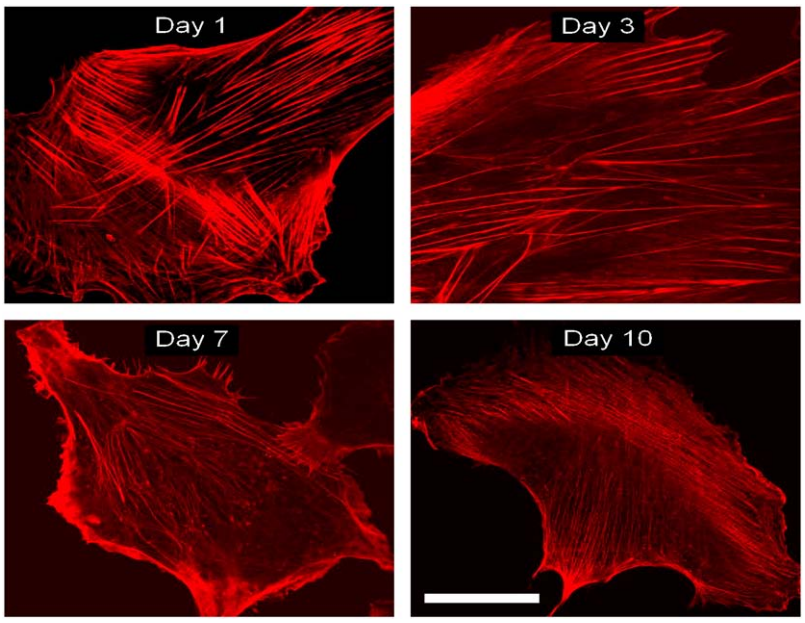

FIGURE 5 Actin cytoskeleton rearrangement during hMSC osteodifferentiation. Within 10 days of osteogenic differentiation induction, more and more thick stress fibers are replaced with a thinner actin filament meshwork typical for mature osteoblasts. Scale bar, 30 μm.

microfilament meshwork filling the cell interior (see Fig. 3). This difference is reflected in cell elasticity: the Young's modulus for hMSCs is twofold higher than that for osteoblasts. Cell stiffness is regulated by actin organization, with microtubules providing only a minor contribution to the cytoskeleton elasticity in both cell types. This result is rather consistent with other studies that suggest that microfilaments and possibly intermediate filaments, but not microtubules, provide the elastic properties of cultured chondrocytes (57). Moreover, microtubules seem not to affect the mechanical properties of either myocytes (58) or fibroblasts (54).

The cytoskeleton appears to affect the mechanical characteristics of another important cell component—the cell plasma membrane, which is known to perform many important functions in cell homeostasis, such as adhesion, motility, endo- and exocytosis, signaling, and metabolic trafficking. Most of these processes are dependent on the membrane surface tension, which is kept constant through several known mechanisms (31), including lipid material recycling, control of membrane rigidity (e.g., by cholesterol content), and interaction with the underlying cytoskeleton (59–61). We have shown previously that the membrane of fibroblasts is tightly bound with the actin cytoskeleton (34). This property might be common for many cells of connective tissue, including osteoblasts, but differs drastically from the weak membrane-cytoskeleton interaction observed in stem cells. Thus, much longer membrane tethers may be produced in hMSCs. Membrane-cytoskeleton adhesion is mediated by transmembrane glycoproteins in the focal contacts, as well as by specific linker proteins (e.g., ezrin, radixin, moesin, myosin-I) that directly attach the membrane to the cytoskeleton (48). Thus, inhibition of the linker proteins by energy depletion has been shown to cause membrane separation from the cell cytoskeleton and subsequent blebbing in renal proximal tubular cells (49). In osteoblasts, either ATP depletion or microfilament depolymerization causes an increase in the membrane tether length extracted with LOT. In contrast, in hMSCs, these treatments do not change the membrane tether characteristics significantly. Apparently, the membrane in stem cells interacts with the cytoskeleton mostly through focal complexes, which were shown to be abundant in these cells (62). In contrast, in mature osteoblasts, in addition to focal adhesions, the membrane is directly bound to the cytoskeleton through multiple protein linkers (Fig. 6). Due to the high density of linker binding sites on the closely packed microfilament network in osteoblasts, the resulting membrane-cytoskeleton interaction is much stronger in osteoblasts than in hMSCs.

We hypothesize that such a drastic difference in mechanical properties is due to specific cell functions. Osteoblasts, fibroblasts, or other connective tissue cells are subjected to multiple mechanical strains and hydraulic-mediated deformations and should withstand such loads without loss of shape or stability. This may be realized by an elastic and compliant cytoskeleton. A thin and dense actin network is ideally suited for this goal, as proven by numerous theoretical models (12,15). On the other hand, one of the main tasks of hMSCs is the ability to respond quickly to the plethora of multifactorial environmental cues by adjusting cell migration, self-renewal, and differentiation activity. All these processes depend substantially on cell adhesion to the extracellular matrix. This could provide an explanation for the many focal adhesion contacts, and strength of adhesion, observed in stem cells. The formation of adhesion focal complexes is associated with the creation of thick actin stress fibers that render the hMSC cytoskeleton very stiff in comparison with that of osteoblasts. In addition, the plasma membrane of hMSCs can adapt for effective signaling through

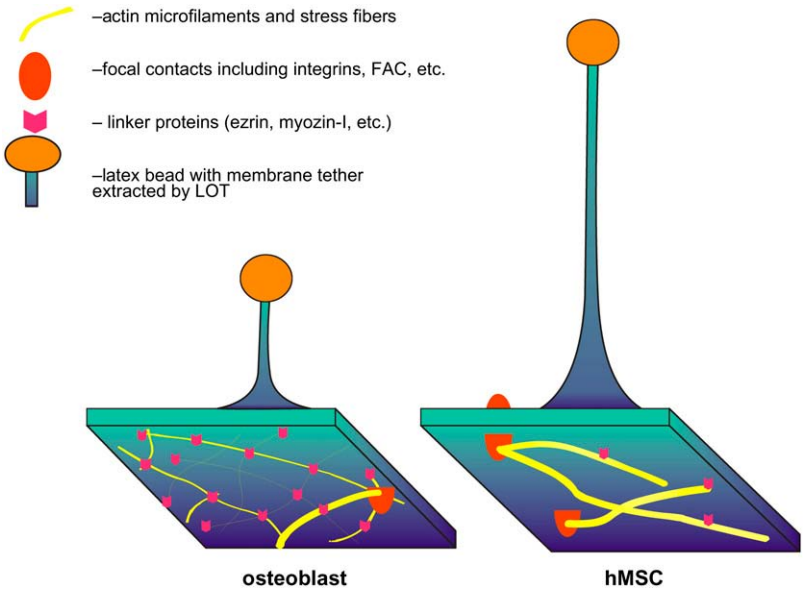

FIGURE 6 Model for the actin cytoskeleton in cellular mechanics of hMSCs and osteoblasts. Thin and dense actin filaments in osteoblasts are tightly bound to the plasma membrane through multiple linker proteins and focal complexes. The hMSC thick stress fibers are associated with the membrane mostly at focal contacts due to a smaller contact area with the membrane and thus lower availability of protein-linker binding sites. As a result, in hMSCs, the overall membrane-cytoskeleton adhesion is weaker and the extracted membrane tether is longer than in osteoblasts. However, the thick-bundled actin structure in hMSCs provides a higher elastic modulus, but a weaker membrane-cytoskeleton interaction, than those found for osteoblasts.

endocytosis and membrane transport, which should be facilitated by the loose binding of the membrane to the cytoskeleton in hMSCs.

During hMSC differentiation into osteoblasts, the mechanics change correspondingly. Both cytoskeleton elasticity and membrane-cytoskeleton adhesion decrease to values similar to those found for mature osteoblasts. Dynamical changes in membrane and cytoskeleton mechanics follow the same temporal pattern (Fig. 4). This result supports the notion that both elasticity and membrane mechanical properties are regulated by the actin cytoskeleton. Although differentiation-induced cytoskeleton reorganization has been reported earlier (63), we describe, for the first time that we know of, the quantitative dynamical characteristics of this process. This dynamics is coherent with other processes taking place in hMSCs during differentiation. For example, after induction of differentiation by the osteogenic soluble factors, intracellular calcium oscillations change immediately (36). Then, upon 3 days in differentiation medium, integrins in the plasma membrane are found to diffuse significantly faster than in normal stem cells (62). Reorganization of the polymeric actin from thick stress fibers into a thinner meshwork is a slower process. The resulting decrease in cell elasticity and increase in membrane-cytoskeleton interaction may be registered by day 7 of differentiation. Finally, after 7–14 days, the specific molecular osteogenic markers are expressed (52). Interestingly, the differentiation dynamics of mechanical parameters appears to depend on the specific lineage of the tissue. For example, we found that a threefold decrease in the hMSC elastic modulus occurred after a 5-day incubation in the neurogenic induction medium (data not shown), compared to a twofold reduction in cytoskeleton elasticity after a 10-day culture in the osteogenic solution. Thus, modulation of cellular mechanics is one of the earlier stages in the biophysical and phenotypic transformation of hMSCs into mature tissue-specific cells.

Such detailed characterization of hMSC mechanics is important for the rapidly growing field of stem-cell-based tissue engineering. A thorough understanding of cellular mechanics will lead to optimal design of biomatrices and scaffolds with specific mechanical properties guiding stem-cell differentiation to a particular lineage. For example, substrate stiffness has been shown to promote cell differentiation into tissue-specific phenotypes, including osteoblasts, myocytes, and neuronal cells (64). Such information will guide the effective use of external physical forces (e.g., electromechanical) to regulate cell differentiation and subsequent integration with developing tissue substitute. More detailed studies would be required to fully explain the role of biomechanics in stem-cell metabolism.

SUMMARY

We have determined the mechanical properties of hMSCs and terminally differentiated bone cells. For the first time that we know of, we have characterized quantitatively the dynamics of stem-cell elasticity and membrane mechanics during osteogenic differentiation. Several mechanical parameters of stem cells appear to be regulated by the actin cytoskeleton, its structure and dynamics. Specifically, osteodifferentiation causes the decrease in cell elasticity and increase in membrane-cytoskeleton interaction that is typical for mature osteoblasts. These modulations are related to remodeling of the actin cytoskeleton from thick stress fibers in hMSCs into the thinner filamentous network in osteoblasts. As biomechanics plays a key role in cellular metabolism, characterization of the mechanical properties of stem cells has great implications for tissue engineering applications and development of new therapies for regenerative medicine.

SUPPLEMENTARY MATERIAL

To view all of the supplemental files associated with this article, visit www.biophysj.org.

This work was supported, in part, by National Institutes of Health grants (GM060741, EB006067) and by a grant from the Office of Naval Research (N00014-06-1-0100).

REFERENCES

1. Kassem, M. 2004. Mesenchymal stem cells: biological characteristics and potential clinical applications. *Cloning Stem Cells.* 6:369–374.
2. Barry, F. P., and J. M. Murphy. 2004. Mesenchymal stem cells: clinical applications and biological characterization. *Int. J. Biochem. Cell Biol.* 36:568–584.
3. Beyer Nardi, N., and L. da Silva Meirelles. 2006. Mesenchymal stem cells: isolation, in vitro expansion and characterization. *Handb. Exp. Pharmacol.* 174:249–282.
4. Settleman, J. 2004. Tension precedes commitment—even for a stem cell. *Mol. Cell.* 14:148–150.
5. Meyers, V. E., M. Zayzafoon, J. T. Douglas, and J. M. McDonald. 2005. RhoA and cytoskeletal disruption mediate reduced osteoblastogenesis and enhanced adipogenesis of human mesenchymal stem cells in modeled microgravity. *J. Bone Miner. Res.* 20:1858–1866.
6. McBeath, R., D. M. Pirone, C. M. Nelson, K. Bhadriraju, and C. S. Chen. 2004. Cell shape, cytoskeletal tension, and RhoA regulate stem cell lineage commitment. *Dev. Cell.* 6:483–495.
7. Yoon, Y., K. Pitts, and M. McNiven. 2002. Studying cytoskeletal dynamics in living cells using green fluorescent protein. *Mol. Biotechnol.* 21: 241–250.
8. Becker, B. E., and D. L. Gard. 2006. Visualization of the cytoskeleton in *Xenopus* oocytes and eggs by confocal immunofluorescence microscopy. *Methods Mol. Biol.* 322:69–86.
9. Ingber, D. E. 2003. Tensegrity I. Cell structure and hierarchical systems biology. *J. Cell Sci.* 116:1157–1173.
10. Stamenovic, D., and N. Wang. 2000. Invited review: engineering approaches to cytoskeletal mechanics. *J. Appl. Physiol.* 89:2085–2090.
11. Volokh, K. Y. 2003. Cytoskeletal architecture and mechanical behavior of living cells. *Biorheology.* 40:213–220.
12. Wang, N., K. Naruse, D. Stamenovic, J. J. Fredberg, S. M. Mijailovich, I. M. Tolic-Norrelykke, T. Polte, R. Mannix, and D. E. Ingber. 2001. Mechanical behavior in living cells consistent with the tensegrity model. *Proc. Natl. Acad. Sci. USA.* 98:7765–7770.

13. Mizuno, D., C. Tardin, C. F. Schmidt, and F. C. Mackintosh. 2007. Nonequilibrium mechanics of active cytoskeletal networks. *Science*. 315:370–373.

14. Stamenovic, D., and D. E. Ingber. 2002. Models of cytoskeletal mechanics of adherent cells. *Biomech. Model. Mechanobiol.* 1:95–108.

15. Lim, C. T., E. H. Zhou, and S. T. Quek. 2006. Mechanical models for living cells—a review. *J. Biomech.* 39:195–216.

16. Ingber, D. E. 2000. Opposing views on tensegrity as a structural framework for understanding cell mechanics. *J. Appl. Physiol.* 89: 1663–1670.

17. Tzima, E. 2006. Role of small GTPases in endothelial cytoskeletal dynamics and the shear stress response. *Circ. Res.* 98:176–185.

18. Knight, M. M., T. Toyoda, D. A. Lee, and D. L. Bader. 2006. Mechanical compression and hydrostatic pressure induce reversible changes in actin cytoskeletal organisation in chondrocytes in agarose. *J. Biomech.* 39:1547–1551.

19. Wang, J. H., and B. P. Thampatty. 2003. An introductory review of cell mechanobiology. *Biomech. Model. Mechanobiol.* 5:1–16.

20. Orr, A. W., B. P. Helmke, B. R. Blackman, and M. A. Schwartz. 2006. Mechanisms of mechanotransduction. *Dev. Cell.* 10:11–20.

21. Ingber, D. E. 2006. Cellular mechanotransduction: putting all the pieces together again. *FASEB J.* 20:811–827.

22. Van Vliet, K. J., G. Bao, and S. Suresh. 2003. The biomechanics toolbox: experimental approaches for living cells and biomolecules. *Acta. Mater.* 51:5881–5905.

23. Huang, H., R. D. Kamm, and R. T. Lee. 2004. Cell mechanics and mechanotransduction: pathways, probes, and physiology. *Am. J. Physiol. Cell Physiol.* 287:C1–11.

24. Bao, G., and S. Suresh. 2003. Cell and molecular mechanics of biological materials. *Nat. Mater.* 2:715–725.

25. Costa, K. D. 2006. Imaging and probing cell mechanical properties with the atomic force microscope. *Methods Mol. Biol.* 319:331–361.

26. Darling, E. M., S. Zauscher, and F. Guilak. 2006. Viscoelastic properties of zonal articular chondrocytes measured by atomic force microscopy. *Osteoarthritis Cartilage.* 14:571–579.

27. Mahaffy, R. E., S. Park, E. Gerde, J. Kas, and C. K. Shih. 2004. Quantitative analysis of the viscoelastic properties of thin regions of fibroblasts using atomic force microscopy. *Biophys. J.* 86:1777–1793.

28. Alcaraz, J., L. Buscemi, M. Grabulosa, X. Trepat, B. Fabry, R. Farre, and D. Navajas. 2003. Microrheology of human lung epithelial cells measured by atomic force microscopy. *Biophys. J.* 84:2071–2079.

29. Togo, T., T. B. Krasieva, and R. A. Steinhardt. 2000. A decrease in membrane tension precedes successful cell-membrane repair. *Mol. Biol. Cell.* 11:4339–4346.

30. Raucher, D., and M. P. Sheetz. 2000. Cell spreading and lamellipodial extension rate is regulated by membrane tension. *J. Cell Biol.* 148: 127–136.

31. Morris, C. E., and U. Homann. 2001. Cell surface area regulation and membrane tension. *J. Membr. Biol.* 179:79–102.

32. Raucher, D., and M. P. Sheetz. 1999. Characteristics of a membrane reservoir buffering membrane tension. *Biophys. J.* 77:1992–2002.

33. Li, Z., B. Anvari, M. Takashima, P. Brecht, J. H. Torres, and W. E. Brownell. 2002. Membrane tether formation from outer hair cells with optical tweezers. *Biophys. J.* 82:1386–1395.

34. Titushkin, I., and M. Cho. 2006. Distinct membrane mechanical properties of human mesenchymal stem cells determined using laser optical tweezers. *Biophys. J.* 90:2582–2591.

35. Dai, J., M. P. Sheetz, X. Wan, and C. E. Morris. 1998. Membrane tension in swelling and shrinking molluscan neurons. *J. Neurosci.* 18:6681–6692.

36. Sun, S., Y. Liu, S. Lipsky, and M. Cho. 2007. Physical manipulation of calcium oscillations facilitates osteodifferentiation of human mesenchymal stem cells. *FASEB J.* (Epub ahead of print.)

37. Hutter, J. L., and J. Bechhoefer. 1993. Calibration of atomic-force microscope tips. *Rev. Sci. Instrum.* 64:1868–1873.

38. Cleveland, J. P., S. Manne, D. Bocek, and P. K. Hansma. 1993. A nondestructive method for determining the spring constant of cantilevers for scanning force microscopy. *Rev. Sci. Instrum.* 64:403–405.

39. Sader, J. E., I. Larson, P. Mulvaney, and L. R. White. 1995. Method for the calibration of atomic-force microscope cantilevers. *Rev. Sci. Instrum.* 66:3789–3798.

40. Harding, J. W., and I. N. Sneddon. 1945. The elastic stresses produced by the indentation of the plane surface of a semi-infinite elastic body by a rigid punch. *Proc. Cambridge Philos. Soc.* 41:16–26.

41. Costa, K. D., and F. C. Yin. 1999. Analysis of indentation: implications for measuring mechanical properties with atomic force microscopy. *J. Biomech. Eng.* 121:462–471.

42. Radmacher, M. 2002. Measuring the elastic properties of living cells by the atomic force microscope. *Methods Cell Biol.* 68:67–90.

43. Mathur, A. B., A. M. Collinsworth, W. M. Reichert, W. E. Kraus, and G. A. Truskey. 2001. Endothelial, cardiac muscle and skeletal muscle exhibit different viscous and elastic properties as determined by atomic force microscopy. *J. Biomech.* 34:1545–1553.

44. Trickey, W. R., F. P. Baaijens, T. A. Laursen, L. G. Alexopoulos, and F. Guilak. 2006. Determination of the Poisson's ratio of the cell: recovery properties of chondrocytes after release from complete micropipette aspiration. *J. Biomech.* 39:78–87.

45. Sneddon, I. N. 1965. The relation between load and penetration in the axisymmetric Boussinesq problem for a punch of arbitrary profile. *Int. J. Eng. Sci.* 3:47–57.

46. Costa, K. D., A. J. Sim, and F. C. Yin. 2006. Non-Hertzian approach to analyzing mechanical properties of endothelial cells probed by atomic force microscopy. *J. Biomech. Eng.* 128:176–184.

47. Hassan, E., W. F. Heinz, M. D. Antonik, N. P. D'Costa, S. Nageswaran, C. A. Schoenenberger, and J. H. Hoh. 1998. Relative microelastic mapping of living cells by atomic force microscopy. *Biophys. J.* 74: 1564–1578.

48. Tsukita, S., and S. Yonemura. 1999. Cortical actin organization: lessons from ERM (ezrin/radixin/moesin) proteins. *J. Biol. Chem.* 274:34507–34510.

49. Chen, J., and M. C. Wagner. 2001. Altered membrane-cytoskeleton linkage and membrane blebbing in energy-depleted renal proximal tubular cells. *Am. J. Physiol. Renal Physiol.* 280:F619–F627.

50. Vaheri, A., O. Carpen, L. Heiska, T. S. Helander, J. Jaaskelainen, P. Majander-Nordenswan, M. Sainio, T. Timonen, and O. Turunen. 1997. The ezrin protein family: membrane-cytoskeleton interactions and disease associations. *Curr. Opin. Cell Biol.* 9:659–666.

51. Algrain, M., O. Turunen, A. Vaheri, D. Louvard, and M. Arpin. 1993. Ezrin contains cytoskeleton and membrane binding domains accounting for its proposed role as a membrane-cytoskeletal linker. *J. Cell Biol.* 120:129–139.

52. Deliloglu-Gurhan, S. I., H. S. Vatansever, F. Ozdal-Kurt, and I. Tuglu. 2006. Characterization of osteoblasts derived from bone marrow stromal cells in a modified cell culture system. *Acta Histochem.* 108:49–57.

53. Pedersen, J. A., and M. A. Swartz. 2005. Mechanobiology in the third dimension. *Ann. Biomed. Eng.* 33:1469–1490.

54. Takai, E., K. D. Costa, A. Shaheen, C. T. Hung, and X. E. Guo. 2005. Osteoblast elastic modulus measured by atomic force microscopy is substrate dependent. *Ann. Biomed. Eng.* 33:963–971.

55. Ricci, D., M. Tedesco, and M. Grattarola. 1997. Mechanical and morphological properties of living 3T6 cells probed via scanning force microscopy. *Microsc. Res. Tech.* 36:165–171.

56. Simon, A., T. Cohen-Bouhacina, M. C. Porte, J. P. Aime, J. Amedee, R. Bareille, and C. Baquey. 2003. Characterization of dynamic cellular adhesion of osteoblasts using atomic force microscopy. *Cytometry A.* 54:36–47.

57. Trickey, W. R., T. P. Vail, and F. Guilak. 2004. The role of the cytoskeleton in the viscoelastic properties of human articular chondrocytes. *J. Orthop. Res.* 22:131–139.

58. Collinsworth, A. M., S. Zhang, W. E. Kraus, and G. A. Truskey. 2002. Apparent elastic modulus and hysteresis of skeletal muscle cells

throughout differentiation. *Am. J. Physiol. Cell Physiol.* 283: C1219–C1227.

59. Sheetz, M. P., J. E. Sable, and H. G. Dobereiner. 2006. Continuous membrane-cytoskeleton adhesion requires continuous accommodation to lipid and cytoskeleton dynamics. *Annu. Rev. Biophys. Biomol. Struct.* 35:417–434.
60. Sechi, A. S., and J. Wehland. 2000. The actin cytoskeleton and plasma membrane connection: PtdIns(4,5)P(2) influences cytoskeletal protein activity at the plasma membrane. *J. Cell Sci.* 113:3685–3695.
61. Sheetz, M. P. 2001. Cell control by membrane-cytoskeleton adhesion. *Nat. Rev. Mol. Cell Biol.* 2:392–396.
62. Chen, H., I. Titushkin, M. Stroscio, and M. Cho. 2007. Altered membrane dynamics of quantum dot-conjugated integrins during osteogenic differentiation of human bone marrow derived progenitor cells. *Biophys. J.* 92:1399–1408.
63. Rodriguez, J. P., M. Gonzalez, S. Rios, and V. Cambiazo. 2004. Cytoskeletal organization of human mesenchymal stem cells (MSC) changes during their osteogenic differentiation. *J. Cell. Biochem.* 93: 721–731.
64. Engler, A. J., S. Sen, H. L. Sweeney, and D. E. Discher. 2006. Matrix elasticity directs stem cell lineage specification. *Cell.* 126: 677–689.